Laser and Particle Beams (2007), *25*, 471–479. Printed in the USA.

DOI: 10.1017/S0263034607000584

High energy self-phase-stabilized pulses tunable in the near-IR by difference frequency generation and optical parametric amplification

C. VOZZI, G. CIRMI, C. MANZONI, E. BENEDETTI, F. CALEGARI, L. LUËR, G. SANSONE, S. STAGIRA, S. DE SILVESTRI, M. NISOLI, AND G. CERULLO

National Laboratory for Ultrafast and Ultraintense Optical Science-CNR—INFM Department of Physics, Politecnico, Milano, Italy

(RECEIVED 14 December 2006; ACCEPTED 22 May 2007)

Abstract

We generate self-phase-stabilized pulses by difference-frequency generation of a hollow-fibre broadened supercontinuum followed by two-stage optical parametric amplification. This system allows the production of broadband pulses widely tuneable in the near-IR wavelength region. Energies up to 0.2 mJ with 15 fs pulse width are demonstrated. These characteristics make this source suitable as a driver for attosecond pulse generation.

Keywords: Difference frequency generation; Optical parametric amplification; Phase stabilization

1. INTRODUCTION

The past few years have seen the growth of attosecond science: due to the impressive progress in the field of driving laser sources, the generation of attosecond pulses by high order harmonic generation (HHG) (Gibson *et al.*, 2003; L'Huillier *et al.*, 2003) has become available, opening the route to the investigation of basic electron processes on a previously unexplored timescale (Kienberger *et al.*, 2004; Agostini & DiMauro, 2004). For the generation of isolated, reproducible attosecond pulses, requirements on the driving pulses are strict: they have to be few-cycle with stable carrier envelope phase (CEP), thus making the electric field completely reproducible (Baltuska *et al.*, 2003; Sola *et al.*, 2006; Sansone *et al.*, 2006). In this paper, we present a novel approach for the generation of high energy, CEP-stabilized, few-optical-cycle pulses widely tuneable in the near-IR wavelength region. The system starts with a passively CEP-stabilized seed produced by difference frequency generation (DFG) between the components of a suitable broadband pulse from a hollow fiber super-continuum (Vozzi *et al.*, 2006). The energy of the seed pulse is then increased up to 0.2 mJ by a two stage optical parametric amplifier (OPA). Pulse duration down to 15 fs, corresponding to about three optical cycles, is demonstrated in the wavelength region around zero dispersion of the system.

The paper is organized as follows: in Section 2, we introduce the application of CEP-stabilized IR pulses to high order harmonic generation and attosecond pulse production. In Section 3, we describe the different approaches to CEP stabilization pointing out the advantage of a passive method based on an intrapulse technique followed by optical parametric amplification for high energy pulse production. In Section 4, we introduce ultra broadband OPAs highlighting their advantages for the generation of high-energy, few-optical-cycle pulses. In section 5, we describe the experimental setup and in Section 6, we present the pulse characterization results. Finally in Section 7, we draw some conclusions with prospects for further developments.

2. HIGH HARMONIC GENERATION WITH FEW-OPTICAL-CYCLE PULSES

High order harmonics are generated during the interaction of a gaseous medium with an intense laser pulse ($I \sim 10^{14}$ W/cm^2). Features of harmonic radiation are nowadays fully understood due to the development of theoretical models like the semiclassical three-step model (Corkum, 1993) and the quantum Lewenstein model for the single atom response to the external laser field (Lewenstein *et al.*, 1994). In the three-step model, the electric field of the driving pulse first ionizes the gas and then accelerates the freed electrons. When the

Address correspondence and reprint requests to: Giulio Cerullo, National Laboratory for Ultrafast and Ultraintense Optical Science - CNR—INFM Department of Physics, Politecnico, Piazza Leonardo da Vinci 32, 20133 Milano, Italy. Email: giulio.cerullo@fisi.polimi.it

direction of the electric field is reversed, the electrons are driven back to the parent ions, and can recombine giving rise to harmonic emission. Obviously the features of harmonic spectrum strongly depend on the driving source. In particular, harmonic radiation is emitted in the form of a train of attosecond pulses, one for each semi-optical cycle of the driving beam. It is possible to isolate a single attosecond pulse either by spectrally selecting the harmonic radiation (Baltuska *et al.*, 2003) or by manipulating the polarization properties of the driving source (Sola *et al.*, 2006; Sansone *et al.*, 2006).

State of the art driving systems for HHG are based on 0.8 μm Ti:Sapphire lasers with chirped-pulse amplification (CPA); pulse duration is reduced by use of the hollow fiber compression technique and the CEP is actively stabilized. As mentioned above, these latter are necessary pre-requisites for attosecond pulse generation. However, 0.8 μm is not the ideal wavelength for the HHG process. This is because the cutoff frequency of harmonic radiation, which means the highest frequency that can be generated in the HHG process, is given by (Lewenstein *et al.*, 1994):

$$\hbar\omega \approx I_P + 3.17U_P, \tag{1}$$

where I_P is the ionization potential of the gas target, and U_P is the ponderomotive energy acquired by the electron in the continuum and it is given by:

$$U_P = \frac{e^2E_0^2}{4m_e\omega_0^2}. \tag{2}$$

In Eq. (2), E_0 and ω_0 represent, respectively, the amplitude, and the frequency of the driving electric field. Thus, the advantage of longer driving wavelengths, results immediately since the ponderomotive energy of the recombining electron increases with the square of the driving pulse wavelength, leading to the generation of higher frequency harmonics; such scaling has been confirmed by a recent theoretical study based on the solution of the time-dependent Schrödinger equation (Tate *et al.*, 2007).

On the other hand, the increment in the carrier wavelength corresponds to a longer transit time for the electron in the continuum, which determines higher diffusion of the electron wavepacket, and reduction in the HHG yield. From the compromise between these effects, it turns out that the ideal driving carrier wavelength would be in the near-IR between 1.5 and 3 μm. These arguments emphasize the interest in developing a high-energy few-optical-cycle driving source in the IR with CEP stabilization. A similar driving source for HHG will allow the generation of harmonic radiation in the soft X region and the generation of reproducible isolated attosecond pulses.

3. CEP STABILIZATION SCHEMES

Ultra broadband light pulses containing only a few optical carrier cycles under their envelope are currently produced by several methods, including direct generation from a mode-locked oscillator (Ell *et al.*, 2001), spectral broadening in a guiding medium (Nisoli *et al.*, 1997), and optical parametric amplification (Baltuska *et al.*, 2002*a*). For such short pulses, the maximum amplitude of the electric field varies significantly between consecutive optical half-cycles, so that it becomes important to control the evolution of the electric field underneath the pulse envelope. The electric field of an ultrashort pulse can be written as

$$E(t) = A(t)\cos(\omega_c t + \phi), \tag{3}$$

where $A(t)$ is the pulse envelope with its maximum at $t = 0$, ω_c is the carrier frequency, and ϕ is the CEP. If $\phi = 0$, a maximum of the electric field corresponds to the peak of the pulse envelope (cosine pulse), while if $\phi = \pi/2$ the electric at the peak of the pulse envelope is zero (sine pulse). Typical femtosecond laser sources generate a pulse train in which the CEP is not stabilized, so that ϕ varies randomly from pulse to pulse. CEP control can be achieved by either active or passive methods, as explained in greater detail in the following.

3.1. Active stabilization

Active CEP stabilization methods rely on the fact that the CEP changes from pulse to pulse in a mode-locked laser oscillator are due to the difference between phase velocity (with which the carrier propagates) and group velocity (with which the envelope propagates) during one roundtrip, so that a systematic pulse to pulse CEP slippage $\Delta\varphi$ occurs at the output of the cavity; in particular, a pulse having phase φ is followed by another with phase $\varphi + 2N\pi + \Delta\varphi$. In order to obtain two pulses with the same CEP, one should therefore wait $2\pi/\Delta\varphi$ roundtrips, so that the so-called carrier-envelope offset (CEO) period is:

$$T_{CEO} = \frac{2\pi}{\Delta\varphi}T_R, \tag{4}$$

where T_R is the roundtrip period in the laser cavity. The corresponding CEO frequency is

$$\nu_{CEO} = \frac{\Delta\phi}{2\pi}\nu_R. \tag{5}$$

Eq. (5) suggests that it is sufficient to pick pulses at frequency ν_{CEO} (or a fraction of it) to generate a train of pulses with reproducible CEP. The two experimental challenges are to measure ν_{CEO} and to stabilize it in time, since it tends to drift due to fluctuations in the cavity parameters. The measurement of ν_{CEO} relies on the fact that a femtosecond mode-locked oscillator emits a frequency comb (Cundiff, 2002; Cundiff & Ye, 2003), i.e., a superposition of longitudinal modes with frequencies:

$$\nu_n = \nu_{CEO} + n\nu_R. \tag{6}$$

https://doi.org/10.1017/S0263034607000584 Published online by Cambridge University Press

The measurement of ν_{CEO} can be performed using a nonlinear *f-2f* interferometer. This instrument requires an input spectrum spanning one optical octave (i.e., with the highest frequency a factor of two larger than the lowest one), which can be obtained directly from the oscillator, or by spectral broadening in a nonlinear fiber. If we now use a second harmonic crystal to frequency double a comb line, with index n, from the low-frequency portion of the spectrum, $\nu_1 = \nu_{CEO} + n\nu_R$, it will have the frequency $2\nu_1 = 2\nu_{CEO} + 2n\nu_R$ which is approximately the same frequency as the comb line on the high-frequency side of the spectrum with index $2n$, $\nu_2 = \nu_{CEO} + 2n\nu_R$. Measuring the heterodyne beat between these yields a difference frequency

$$2\nu_1 - \nu_2 = 2\nu_{CEO} + 2n\nu_R - (\nu_{CEO} + 2n\nu_R) = \nu_{CEO}, \qquad (7)$$

which is the sought after CEO frequency. Once ν_{CEO} is measured, it can be stabilized by active feedback on the oscillator. The selected CEP-stable pulses at a fraction of ν_{CEO} can then amplified either in a solid-state amplifier (Baltuska *et al.*, 2003) or in an OPA (Hauri *et al.*, 2004; Zinkstok *et al.*, 2005); a second electronic feedback loop is required to compensate for the slow CEP fluctuations induced by the amplification process. Actively CEP-stabilized few-optical-cycle pulses are currently produced by amplified Ti:Sapphire systems and display rms CEP fluctuations of the order of 0.1 rad.

3.2. Passive stabilization

A completely different approach for the generation of CEP stable pulses is the passive one, which relies on nonlinear optical processes to cancel the pulse-to-pulse CEP fluctuations. In order to understand the principles of this method, it is useful to consider the effects of various nonlinear processes on the CEP, as summarized in Table 1.

In the third-order process of self-phase modulation (SPM), the CEP is preserved, and shifted by a constant amount of $\pi/2$. In the second-order process of sum-frequency generation (SFG), in which two pulses at frequencies ω_1 and ω_2, with CEPs ϕ_1 and ϕ_2, are mixed in a nonlinear crystal to generate the sum frequency $\omega_3 = \omega_1 + \omega_2$, the CEP of the resulting pulse is $\phi_3 = \phi_1 + \phi_2 + \pi/2$. For the particular case of second harmonic generation (SHG) starting from a pulse with frequency ω and CEP φ one obtains a pulse with frequency 2ω and CEP $2\varphi + \pi/2$. In the second-order process of DFG between two pulses at frequencies ω_2 and ω_3, with CEPs ϕ_2 and ϕ_3, the resulting difference frequency (DF) pulse has frequency $\omega_1 = \omega_3 - \omega_2$ and CEP $\phi_1 = \phi_3 - \phi_2 - \pi/2$. In the similar process of OPA, an intense high-energy pump pulse, at frequency ω_3, amplifies a weak signal pulse at frequency ω_2, thereby generating an idler pulse at $\omega_1 = \omega_3 - \omega_2$. In this case, the amplification process preserves the CEP of the signal, while that of the idler is given by $\phi_1 = \phi_3 - \phi_2 - \pi/2$, as in the DFG process.

Table 1. *Effects of the main nonlinear processes on absolute phase*

	Input Pulses		Output pulses	
Process	Frequencies	CEP	Frequencies	CEP
SPM	ω	ϕ	ω	$\phi + \pi/2$
SFG	ω_1,ω_2	ϕ_1,ϕ_2	$\omega_1 + \omega_2$	$\phi_1 + \phi_2 + \pi/2$
SHG	ω	ϕ	2ω	$2\phi + \pi/2$
DFG	ω_3,ω_1	ϕ_3,ϕ_1	$\omega_3 - \omega_1$	$\phi_3 - \phi_1 - \pi/2$
OPA	ω_3,ω_1	ϕ_3,ϕ_1	ω_1	ϕ_1

With these relationships at hand, we can now understand the passive CEP stabilization approach: if the two pulses undergoing the DFG process share the same CEP ($\phi_3 = \phi + c_3$, $\phi_2 = \phi + c_2$), then $\phi_1 = c_3 - c_2 - \pi/2 = \text{const.}$, i.e., the fluctuations of ϕ are automatically cancelled in a passive, all-optical way (Baltuska *et al.*, 2002*b*). Passive CEP stabilization has some clear advantages with respect to the active one: (1) it is an all-optical technique and does not require any electronic feedback circuits; (2) it directly produces a train of CEP-stable pulses, avoiding the need to pick pulses at a fraction of ν_{CEO}. There are several possible experimental implementations of this method. *Inter-pulse* DFG processes involve mixing of two separate frequency-shifted pulses, synchronized by a delay line, as schematically represented in Figure 1a. In this case, any fluctuation of the path-length difference, due to mechanical instabilities or air turbulences, will induce a CEP jitter on the DF pulses. A more robust approach is based on an *intra-pulse* scheme, in which DFG is achieved between long and short wavelength components of a single ultra broadband pulse, as represented in Figure 1b (Fuji *et al.*, 2004, 2005). In this case, the DFG occurs between different spectral portions of the same

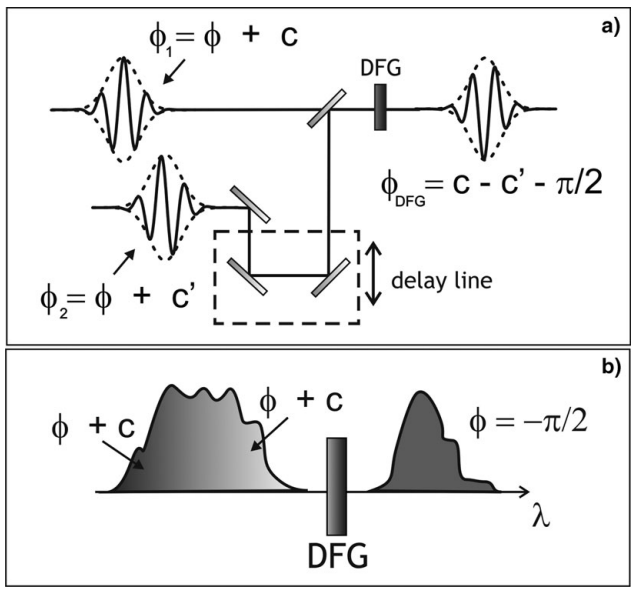

Fig. 1. *interpulse* (**a**) and *intrapulse* (**b**) schemes for passive CEP stabilization through difference frequency generation.

https://doi.org/10.1017/S0263034607000584 Published online by Cambridge University Press

pulse and delay-induced CEP jitter is suppressed. Moreover, synchronization is automatically achieved by controlling the group delay of the pulse.

CEP-stable pulses by inter-pulse DFG are naturally produced by an OPA; if pump and signal are derived from the same laser source and thus share the same CEP, the idler is phase stable. This can be realized starting both from the fundamental frequency (FF) or the second harmonic (SH) of an amplified laser source, typically a CPA Ti:Sapphire laser (Fang & Kobayashi, 2004; Adachi *et al.*, 2004). Generation of CEP-stable pulses directly from an OPA has the drawback that few-optical-cycle idler pulses can be obtained only by operating the OPA in broadband configurations. OPAs provide broad gain bandwidth when operated around degeneracy (for type I phase matching) in a collinear geometry or, for a blue pump, in the non-collinear geometry with a suitable angle (Cerullo & De Silvestri, 2003). These designs show experimental disadvantages: in a collinear type I OPA at degeneracy, both signal and idler lie in the same broadband spectral region, they share the same polarization, and travel along the same direction, preventing the separation of the phase-unstable signal from the CEP-stabilized idler. On the other hand, in the non-collinear configuration the idler beam is angularly dispersed due to momentum conservation, and sophisticated optical systems are required to recombine its different colors (Shirakawa *et al.*, 1998). Other inter-pulse configurations exploit the DFG process between broadband pulses generated by two OPAs sharing the same CEP. By choosing a Type II collinear configuration, it is possible to obtain broadband DF pulses in the infrared spectral region, albeit with low energy (Manzoni *et al.*, 2004). Recently, the CEP-stable idler of a narrowband near-IR OPA was spectrally broadened in a sapphire plate and used to seed a broadband non-collinear OPA, thus producing few-optical-cycle CEP stable visible pulses (Manzoni *et al.*, 2007). In another experiment, the CEP-stable idler of a near-IR OPA was spectrally broadened and self-compressed by filamentation, producing 270-μJ, 18-fs CEP-stable pulses at 2 μm (Hauri *et al.*, 2007).

Intra-pulse stabilization schemes have also been experimentally implemented. In a first configuration, pulses generated by DFG from an ultra broadband Ti:Sapphire oscillator were stretched, and used to seed an optical parametric chirped pulse amplifier pumped by an electronically synchronized 40 ps Nd:YLF laser; the system produces 20-fs, 80-μJ phase stable pulses at 2.1 μm (Fuji *et al.*, 2006). We have recently proposed a different configuration, which is driven by a CPA Ti:Sapphire system; the pulses generated by this laser, with random CEP, are spectrally broadened in a hollow-fiber and undergo intrapulse DFG, thus generating broadband, CEP-stable near-IR pulses. The low-energy seed pulses are then amplified by two OPA stages, pumped by the FF of Ti:Sapphire, and operated around degeneracy. In an initial implementation of this scheme,we generated 20-μJ CEP-stable pulses (Manzoni *et al.*, 2006) around 1.2 μm. Here we report on the energy scaling of this source by one order of magnitude, to generate tuneable near-IR pulses with energy up to 200 μJ and pulse duration down to 15 fs.

4. HIGH ENERGY, ULTRA BROADBAND OPTICAL PARAMETRIC AMPLIFIERS

OPAs are normally used to add tunability to an otherwise fixed-wavelength source. They have however other advantages, with respect to standard amplifiers based on population inversion in an active material, that make them attractive for the generation of few-optical-cycle high-energy pulses. OPAs are often the method of choice for scaling the pulse energy because: (1) they have the capability of providing a high gain in a relatively short path length, allowing a compact, tabletop amplifier setup and also minimizing the linear and non-linear phase distortions and ensuring an excellent temporal and spatial quality of the pulses; (2) amplification occurs only during the pump pulse, so that the amplified spontaneous emission and the consequent prepulse pedestal are greatly reduced; (3) in a standard amplifier, even for good energy extraction, there is always some thermal loading, due to the quantum defect (difference between energies of the pump and emitted photons, usually absorbed by the material in non-radiative decay processes); this becomes very relevant for high energy amplifiers, often requiring cryogenic cooling. In an OPA, on the other hand, no fraction of the pump photon energy is deposited in the medium, because it is transformed in the sum of the signal and idler photon energies; so thermal loading effects, apart from parasitic absorption, are completely absent, greatly reducing spatial aberration effects on the beams.

In addition to these advantages for efficient high-energy generation, the OPA has also the capability to sustain very broad amplification bandwidths, allowing the generation of few-optical-cycle pulses (Cerullo & De Silvestri, 2003). This is due to the fact that amplification efficiency depends on phase-matching condition $\Delta k = k_{\mathrm{p}} - k_{\mathrm{s}} - k_{\mathrm{i}} = 0$, where k_{p}, k_{s}, and k_{i} are pump, signal and idler wave vectors respectively. In particular, the gain bandwidth of an OPA can be written to the first order as

$$\Delta\nu = \frac{2(\ln 2)^{1/2}}{\pi}\left(\frac{\Gamma}{L}\right)^{1/2}\frac{1}{\left|1/v_{gi} - 1/v_{gs}\right|}, \tag{8}$$

where L is the crystal length, v_{gs} and v_{gi} are the group velocities of signal and idler, respectively, and $\Gamma^2 = 2d_{eff}^2\omega_i\omega_s/c_0^3\varepsilon_0 n_i n_s n_p I_p$, where I_p is the pump intensity, and d_{eff} is the second-order nonlinear coefficient of the crystal. Eq. (8) suggests that broadband operation is achieved by group velocity matching between signal and idler pulses; this occurs around degeneracy ($\omega_s = \omega_i = \omega_p/2$) when signal and idler propagate with parallel polarization (type I phase matching). For this reason, FF-pumped OPAs generate ultra broadband pulses around 1.6 μm, while SH pumped OPAs generate ultra broadband pulses around 800 nm; in the visible spectral range the IR idler pulses propagate with higher group

https://doi.org/10.1017/S0263034607000584 Published online by Cambridge University Press

velocities than the signal so that only narrowband amplification is possible. In spectral regions different from degeneracy, broadband operation requires non-collinear interaction geometry, in which pump, signal, and idler propagate along different directions. By calculating phase matching as a vector equation, one finds that the angle between signal and pump wave vectors necessary for broadband operation is chosen in such a way that the projection of the idler group velocity along the signal direction equals the signal group velocity.

5. EXPERIMENTAL SETUP

A scheme of the experimental setup is given in Figure 2a. The laser source is a Ti:Sapphire-based system producing 50-fs, 1.5-mJ, 1-kHz pulses and centered at 800 nm. 0.25-mJ have been spectrally broadened in a 60-cm-long hollow fiber (300 μm inner diameter) filled with krypton (Nisoli *et al.*, 1996, 1997). The output pulses, with energy up to 0.2-mJ, were compressed by chirped mirrors down to 12 fs; the pulses were also given a slightly negative chirp in order to optimize the DF process. Such driving pulses were then focused by a spherical mirror (radius of curvature, R = 1500 mm) on a 200-μm thick β-barium borate (BBO) crystal; the position of this crystal with respect to the beam waist was adjusted in order to keep the intensity of the driving pulses below the threshold for the onset of third-order nonlinear processes.

The understanding of intra-pulse DFG process and the choice of the best nonlinear crystal is not straightforward, since this process takes place between many components of the broadband driving pulse. We can first assume that a DF photon at ω_i is generated after the interaction between a spectral component beyond 700 nm (pump, at frequency ω_p) and one with wavelength longer than 800 nm (signal, at frequency ω_s). In this case, the efficiency and bandwidth of the process can be evaluated by studying the phase-matching condition $k_p - k_s - k_i = 0$ for all of the possible pairs of interacting pump and signal wavelengths. Figure 3 shows the phase-matched components of the broadband hollow-fiber driving pulse for two different Type II interaction schemes ($e + o$[DFG] $\rightarrow e$ and $o + e$[DFG] $\rightarrow e$) in BBO crystal. The curves are given for various crystal cuts θ; dashed gray lines show the DF wavelengths, and their intersections with the phase-matching curves give the

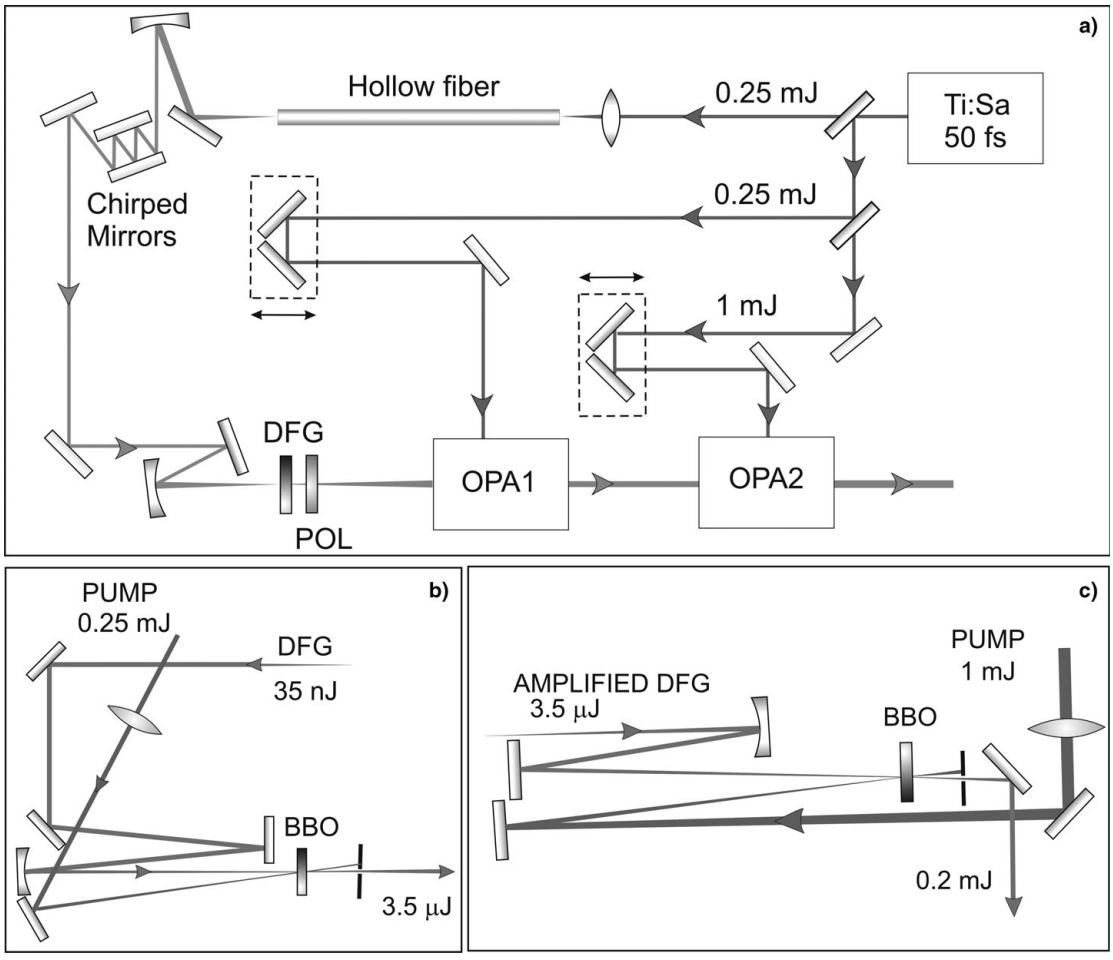

Fig. 2. (**a**) Experimental setup for the generation of high-energy self-phase-stabilized pulses. (**b**) Layout of the first OPA. (**c**) Layout of the second OPA. Ti:Sa, CPA Ti:Sapphire laser; DFG, 2 micron thick BBO crystal; POL, thin film polarizer.

https://doi.org/10.1017/S0263034607000584 Published online by Cambridge University Press

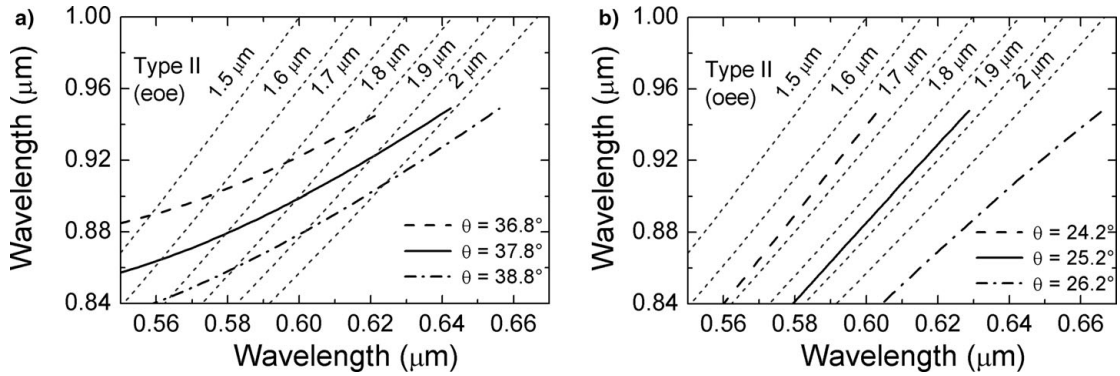

Fig. 3. Phase-matched wavelengths obtained exploiting (**a**) Type II (eoe) and (**b**) Type II (oee) configurations. Dashed lines give the DF wavelengths.

phase-matched DF frequencies. Figure 3a shows that Type II (eoe) allows generating broadband DF pulses, with spectrum ranging from 1.5 to 2 μm, since a single value of θ intersects a broad range of DF wavelengths; on the other hand, the curves on the right panel indicate that the Type II (oee) process gives only narrowband pulses, since only a narrow range of DF frequencies can be phase-matched for a given value of θ, and it is thus not suitable for the generation of few-optical-cycle CEP-stable pulses. Type I interaction ($o + o[\mathrm{DFG}] \rightarrow e$) is not suitable for intra-pulse DFG because phase matching is much more involved, since several pairs of frequencies can generate the same DF frequency, making CEP stabilization more difficult to handle. In addition spurious SHG processes take place, which may spoil the DFG interaction. According to this analysis, we used BBO crystal cut for Type II (eoe) phase matching: the broadband beam from the hollow fiber was polarized along the extraordinary plane of the nonlinear crystal and gave DF pulses with ordinary polarization. The bandwidth and central frequency of the generated DF pulses were finely tuned by controlling the crystal phase-matching angle and optimizing the chirp of the driving pulse by a couple of thin fused silica wedges. Typical energy value of the DF signal was 20 nJ; the ordinarily polarized DF could be separated from the driving pulse with a polarizer due to the different polarization of the beams. As shown in Figure 4, typical DF spectra were tunable in the whole detectable range between 1.2 and 2.4 μm with near single-cycle transform limited (TL) pulse duration.

To boost in energy the generated DF signal, we developed a two-stage OPA pumped by the residual 800-nm beam. The first stage is shown in Figure 2b: 0.25-mJ pump pulses drive a 2-mm-thick BBO crystal cut for type I phase matching ($\theta = 21^\circ$, $\phi = 0^\circ$). This first amplifier produces pulses with energy up to 3.5 μJ, and a spectrum almost as broad as that of the DF pulses (dashed line in Fig. 5), as expected from a type I OPA operated around degeneracy (Cerullo & De Silvestri, 2003). The second OPA stage is pumped by 1 mJ FF pulses and uses a 3-mm-thick BBO crystal cut for type II phase matching ($\theta = 28.5^\circ$, $\varphi = 30^\circ$); the reduced gain bandwidth of this configuration allows one to obtain a narrower amplified pulse spectrum, which is less sensitive to uncompensated chirp, and gives pulses closer to TL duration. When driven into saturation, the second OPA stage generates pulses

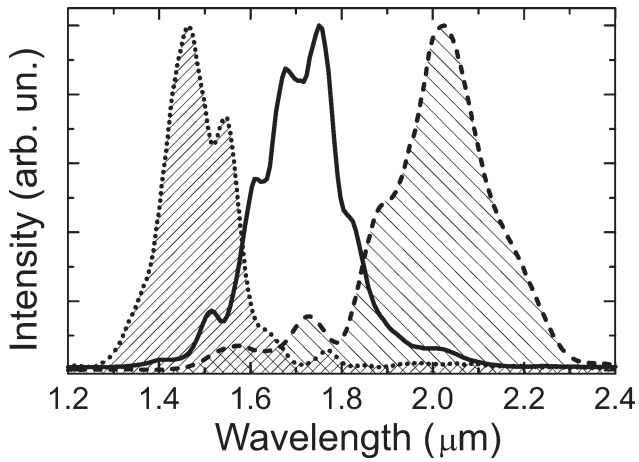

Fig. 4. Spectra of the DF signal. Different curves correspond to different phase-matching conditions.

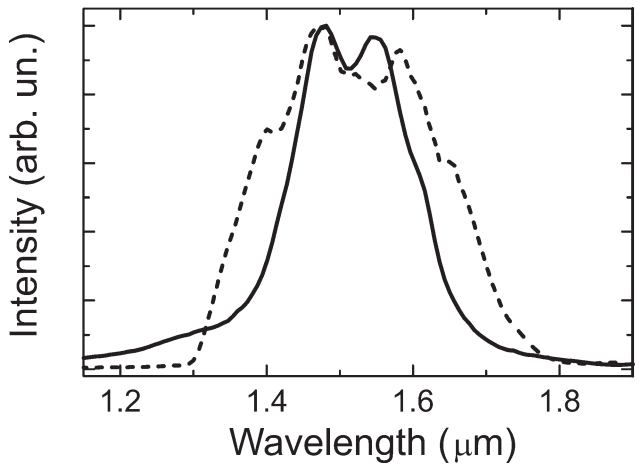

Fig. 5. Spectra of the pulses after the first (dashed line) and the second (solid line) OPA.

https://doi.org/10.1017/S0263034607000584 Published online by Cambridge University Press

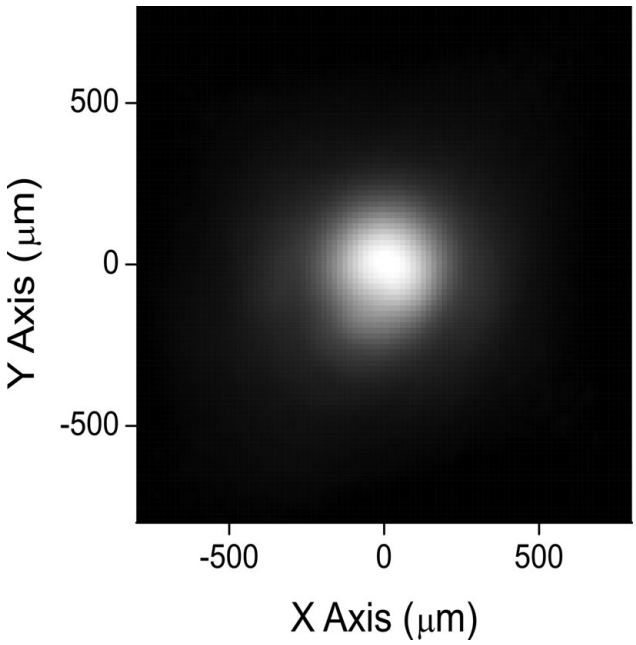

Fig. 6. Intensity profile of the DF signal after the second OPA stage.

with 0.2-mJ energy, which, taking into account the idler energy, corresponds to a 40% overall pump conversion efficiency. Due to gain saturation, the pulse spectrum, shown in Figure 5 (solid line), is only slightly narrower than the one of the first stage. In both OPA stages, we used a non-collinear geometry with a small angle (≈1.5°) between pump and seed to facilitate combination and separation of the beams and to prevent signal-idler interference. They were also operated in a regime in which parametric superfluorescence was negligible once the DF seed is blocked. It is worth noting that minimizing the superfluorescence background is of crucial importance for CEP stabilization, since this background is not phase-stabilized, and thus degrades the CEP stability of the DF signal.

6. PULSE CHARACTERIZATION

The generated pulses are characterized by excellent energy stability due to the saturation of the second OPA: we measured a peak-to-peak root mean squared (rms) fluctuation of less than 4%. The very good spatial quality of the beam was measured with a CCD camera and is shown in Figure 6.

We also measured the time duration of DF pulses after the second OPA with unbalanced interferometric autocorrelation. It is worth noting that we would expect nearly transform limited pulse duration, since the DFG process does not introduce chirp, and the BBO crystals present zero order dispersion around 1.4 μm. By tuning the carrier wavelength of DF signal around this value, the total dispersion introduced by the system remained negligible. The autocorrelation measurement is shown in Figure 7 (dots); the corresponding spectrum is reported in the inset. For evaluating the pulse duration, the measurement is compared with a

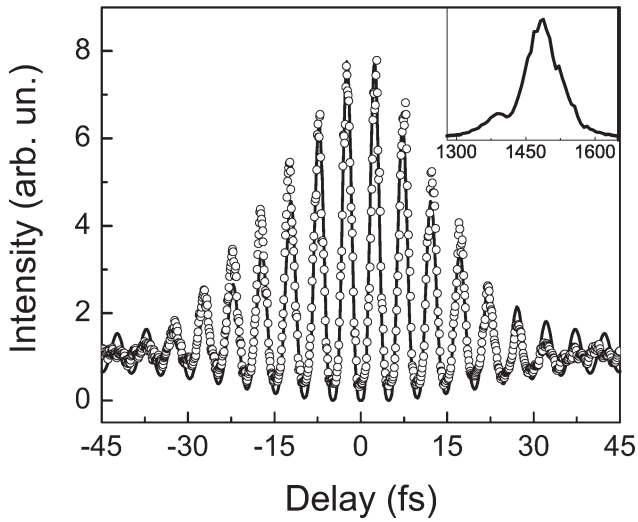

Fig. 7. Measured interferometric autocorrelation of the high-energy pulses (thick solid line) and calculated autocorrelation (thin solid line) starting from the pulse spectrum (shown in the inset) and assuming flat spectral phase.

calculated interferometric trace (solid line in Fig. 7) obtained from the actual spectrum and assuming flat spectral phase. This comparison implies a nearly transform limited FWHM pulse duration of 15 fs, which corresponds to less than 3 optical cycles at the carrier frequency.

The stability of the CEP was also verified with a *f*-to-2*f* interferometer (Kakehata *et al.*, 2001) in which a small

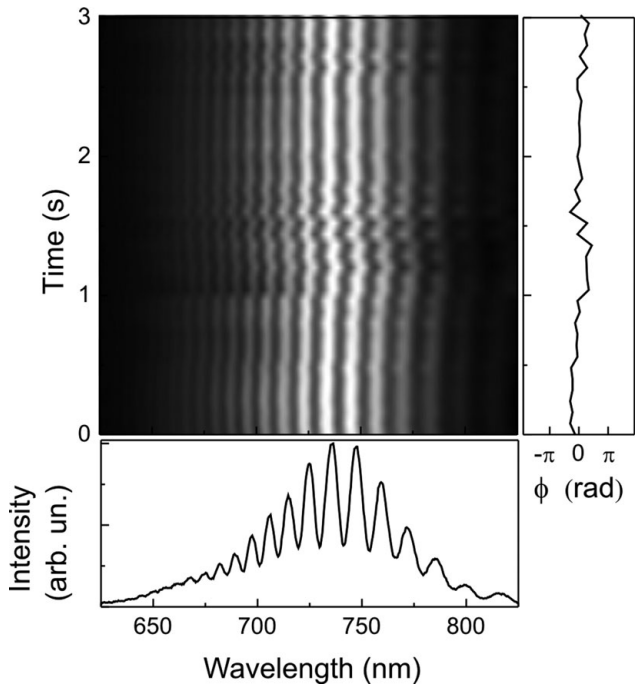

Fig. 8. Upper left panel: sequence of interferograms acquired with the *f-to-2 f* interferometer over successive laser shots. Each interferogram corresponds to 5 pulses, one interferogram is shown in the lower left panel. Right panel: mean value of the phase slip reconstructed from the interferograms.

https://doi.org/10.1017/S0263034607000584 Published online by Cambridge University Press

fraction of the amplified DF signal was focused on a sapphire plate for spectral broadening through super continuum generation and then was frequency doubled in a thin BBO crystal and sent to a spectrometer through a polarizer. The white light produced in the sapphire plate interfered with the second harmonic of the driving DF signal in the spectral region around 750 nm. The appearance of a stable interference pattern guaranteed the CEP stability. Figure 8 shows a sequence of interference patterns acquired for 3 s; each interferogram results from the average between five shots. The rms for the CEP drift calculated for this series of measurements is 0.5 rad and it indicates some residual fluctuation which can be due to amplitude-to-phase coupling in the super continuum generation process or environmental noise.

7. CONCLUSIONS

We have demonstrated the possibility to generate CEP-stabilized pulses by DFG driven by a hollow fiber broadened super continuum. By amplification in two OPA stages, energy up to 0.2 mJ with near transform limited pulse duration of 15 fs has been achieved. This passive approach to CEP stabilization is intrinsically robust since it is based on the reliable CPA Ti:Sapphire laser systems and it is an all-optical method. In addition this technique is capable to generate pulses easily tuneable in a wide spectral range in the near-IR by changing phase-matching conditions. These characteristics make this source particularly suitable as a driver for HHG experiments. Further optimization of this system can be realized by changing the crystal of the second OPA to a type I configuration thus exploiting the broad phase-matching bandwidth of the first OPA; in this case a gain bandwidth supporting a sub 10 fs pulse duration should be possible, as demonstrated by the first stage. Such broadband pulses would require a suitable compressor stage to achieve a transform-limited duration. Since we are working close to the zero second order dispersion wavelength of BBO the compressor should compensate mainly the third order dispersion. A simple setup based on a deformable mirror should give the spectral phase correction necessary to achieve near single cycle pulses. Such pulses would be ideal drivers for the generation of single attosecond pulses by HHG.

ACKNOWLEDGEMENT

We acknowledge the experimental support of Daniele Brida. This work was partially supported by the European Union within contracts RII3-CT-2003-506350 (Laserlab Europe) and MRTNCT-2003-505138 (XTRA).

REFERENCES

Adachi, S., Kumbhakar, P. & Kobayashi, T. (2004). Quasi-monocyclic near-infrared pulses with a stabilized carrier-envelope phase characterized by noncollinear cross-correlation frequency-resolved optical gating. *Opt. Lett*. **29**, 1150–1152.

Agostini, P. & DiMauro, L.F. (2004). The physics of attosecond light pulses. *Rep. Prog. Phys.* **67**, 813–855.

Baltuska, A., Fuji, T. & Kobayashi, T. (2002*a*). Visible pulse compression to 4 femtoseconds by optical parametric amplification and programmable dispersion control. *Opt. Lett*. **27**, 306–308.

Baltuska, A., Fuji, T. & Kobayashi, T. (2002*b*). Controlling the carrier-envelope phase of ultrashort light pulses with optical parametric amplifiers. *Phys. Rev. Lett*. **88**, 133901–133904.

Baltuska, A., Udem, T., Uiberacker, M., Hentschel, M., Goulielmakis, E., Gohle, C., Holzwarth, R., Yakovlev, V.S., Scrinzi, A., Hansch, T.W. & Krausz, F. (2003). Attosecond control of electronic processes by intense light field. *Nature* **421**, 611–615.

Cerullo, G. & De Silvestri, S. (2003). Ultrafast optical parametric amplifiers. *Rev. Sci. Instrum*. **74**, 1.

Corkum, P.B. (1993). Plasma perspectives on strong-field multiphoton ionization. *Phys. Rev. Lett.* **71**, 1994.

Cundiff, S.T. & Ye, J. (2003). *Colloquium*: Femtosecond optical frequency combs. *Rev. Mod. Phys*. **75**, 325–342.

Cundiff, S.T. (2002). Phase stabilization of ultrashort optical pulses. *J. Phys. D: Appl. Phys*. **35**, 43–59.

Ell, R., Morgner, U., Kaertner, F.X., Fujimoto, J.G., Ippen, E.P., Scheuer, V., Angelow, G., Tschudi, T., Lederer, M.J., Boiko, A. & Luther-Davis, B. (2001). Generation of 5-fs pulses and octave-spanning spectra directly from a Ti:sapphire laser. *Opt. Lett*. **26**, 373–375.

Fang, X. & Kobayashi, T. (2004). Self-stabilization of the carrier-envelope phase of an optical parametric amplifier verified with a photonic crystal fiber. *Opt. Lett*. **29**, 1282–1284.

Fuji, T., Apolonski, A. & Krausz, F. (2004). Self-stabilization of carrier-envelope offset phase by use of difference-frequency generation. *Opt. Lett*. **29**, 632–634.

Fuji, T., Ishii, N., Teisset, C.Y., Gu, X., Metzger, T., Baltuska, A., Forget, N., Kaplan, D., Galvanauskas, A. & Krausz, F. (2006). Parametric amplification of few-cycle carrier envelope phase-stable pulses at 2.1 μm. *Opt. Lett*. **31**, 1103–1105.

Fuji, T., Rauschenberger, J., Apolonski, A., Yakovlev, V., Tempea Udem, G.T., Gohle, C., Haensch, T., Lehnert, W., Scherer, M. & Krausz, F. (2005). Monolithic carrier envelope phase-stabilization scheme. *Opt. Lett.* **30**, 332–334.

Gibson, E.A., Paul, A., Wagner, N., Tobey, R., Gaudiosi, D., Backus, S., Christov, I.P., Aquila, A., Gullikson, E.M., Attwood, D.T., Murnane, M.M. & Kapteyn, H.C. (2003). Coherent soft X-ray generation in the water window with quasi-phase matching. *Science* **302**, 95–98.

Hauri, C., Schlup, P., Arisholm, G., Biegert, J. & Keller, U. (2004). Phase-preserving chirped-pulse optical parametric amplification to 17.3 fs directly from a Ti:sapphire oscillator. *Opt. Lett*. **29**, 1369–1371.

Hauri, C.P., Lopez-Martens, R.B., Blaga, C.I., Schultz, K.D., Cryan, J., Chirla, R., Colosimo, P., Doumy, G., March, A.M., Roedig, C., Sistrunk, E., Tate, J., Wheeler, J. & DiMauro, L.F. (2007). Intense self-compressed, self-phase-stabilized few-cycle pulses at 2 μm from an optical filament. *Opt. Lett.* **32**, 868–870.

Kakehata, M., Takada, H., Kobayashi, Y., Torizuka, K., Fujihara, Y., Homma, T. & Takahashi, H. (2001). Single-shot measurement of carrier-envelope phase changes by spectral interferometry. *Opt. Lett*. **26**, 1436–1438.

Kienberger, R., Goulielmakis, E., Uiberacker, M., Baltuska, A., Yakovlev, V., Bammer, F., Scrinzi, A., Westerwalbesloh, Th.,

Kleineberg, U., Heinzmann, U., Drescher, M. & Krausz, F. (2004). Atomic transient recorder. *Nature* **427**, 817–821.

Lewenstein, M., Balcou, Ph., Yu, Ivanov, M., L'Huillier, A. & Corkum, P.B. (1994). Theory of high-harmonic generation by low-frequency laser fields *Phys. Rev. A* **49**, 2117–2132.

L'Huillier, A., Descamps, D., Johansson, A., Norin, J., Mauritsson, J. & Wahlstrom, C.-G. (2003). Applications of high order harmonics. *Eur. Phys. J. D* **26**, 91–98.

Manzoni, C., Cerullo, G. & De Silvestri, S. (2004). Ultrabroadband self-phase-stabilized pulses by difference-frequency generation. *Opt. Lett*. **29**, 2668–2670.

Manzoni, C., Polli, D., Cirmi, G., Brida, D., De Silvestri, S. & Cerullo, G. (2007). Tunable few-optical-cycle pulses with passive carrier-envelope phase stabilization from an optical parametric amplifier. *Appl. Phys. Lett.* **90**, 171111.

Manzoni, C., Vozzi, C., Benedetti, E., Sansone, G., Stagira, S., Svelto, O., De Silvestri, S., Nisoli, M. & Cerullo, G. (2006). Generation of high energy self-phase stabilized pulses by difference frequency generation followed by optical parametric amplification. *Opt. Lett*. **31**, 963–965.

Nisoli, M., De Silvestri, S. & Svelto O. (1996). Generation of high energy 10 fs pulses by a new pulse compression technique. *Appl. Phys. Lett*. **68**, 2793–2795.

Nisoli, M., De Silvestri, S., Svelto, O., Szipocs, R., Ferencz, K., Spielmann, Ch., Sartania, S. & Krausz, F. (1997). Compression of high-energy laser pulses below 5 fs. *Opt. Lett.* **22**, 522–524.

Sansone, G., Benedetti, E., Calegari, F., Vozzi, C., Avaldi, L., Flammini, R., Poletto, L., Villoresi, P., Altucci, C., Velotta, R., Stagira, S., De Silvestri, S. & Nisoli, M. (2006). Isolated single-cycle attosecond pulses. *Science* **314**, 443–446.

Shirakawa, A. Sakane, I. & Kobayashi, T. (1998). Pulse-front-matched optical parametric amplification for sub-10-fs pulse generation tunable in the visibile and near-infrared. *Opt. Lett*. **23**, 1292–1294.

Sola, I.J., Mevel, E., Elouga, L., Constant, E., Strelkov, V., Poletto, L., Villoresi, P., Benedetti, E., Caumes, J.-P., Stagira, S., Vozzi, C., Sansone, G. & Nisoli, M. (2006). Controlling attosecond electron dynamics by phase-stabilized polarization gating. *Nature Phys.* **2**, 319–322.

Tate, J., Auguste, T., Muller, H.G., Salieres, P., Agostini, P. & Dimauro, L.F. (2007). Scaling of wave-packet dynamics in an intense midinfrared field *Phys. Rev. Lett.* **98**, 013901–013904.

Vozzi, C., Cirmi, G., Manzoni, C., Benedetti, E., Calegari, F., Sansone, G., Stagira, S., Svelto, O., De Silvestri, S., Nisoli, M. & Cerullo, G. (2006). High-energy, few-optical cycle pulses at 1.5 μm with passive carrier-envelope phase stabilization *Opt. Exp.* **14**, 10109–10116.

Zinkstok, R., Witte, S., Hogervorst, W. & Eikema, K. (2005). High-power parametric amplification of 11.8-fs laser pulses with carrier-envelope phase control. *Opt. Lett*. **30**, 78–80.

https://doi.org/10.1017/S0263034607000584 Published online by Cambridge University Press